ELSEVIER

7 July 1997

PHYSICS LETTERS A

Physics Letters A 231 (1997) 231-234

Electron scattering by SF_6 molecules at intermediate energies

Yuhai Jiang, Jinfeng Sun, Lingde Wan

CCAST (World Laboratory), P.O. Box 8730, Beijing 100080, China

Department of Physics, Henan Normal University, Xinxiang, Henan 453002, China [1]

Received 4 February 1997; revised manuscript received 24 April 1997; accepted for publication 25 April 1997
Communicated by B. Fricke

Abstract

We report the first calculations of the elastic differential cross sections (DCS) for electron scattering from SF_6 at six impact energies (in the range 100–700 eV) employing the independent atom model (IAM) with partial waves. The atoms are presented by a model complex optical potential which is composed of static, exchange, polarization, and absorption terms. The integrated elastic and momentum transfer cross sections are obtained. Compared with available experimental data, the present approach presents good results. © 1997 Elsevier Science B.V.

PACS: 34.80.B

SF_6 molecules have been widely used as an insulation gas in high-voltage equipment and its differential cross sections (DCS), integrated elastic and momentum transfer cross sections for electron scattering have important applications in space, atmospheric, plasma, and chemistry physics [1]. It is well known that electron–molecule scattering presents a more complex problem than the corresponding electron–atom scattering due to its multicentre nature, lack of a center of symmetry (in the case of polyatomic and hetero-nuclear molecules) and nuclear motion. Here we are interested in the intermediate- and high-energy region, where almost all inelastic channels (rotational, vibrational, and electronic excitation, ionization processes, etc.) are open. In this energy range, since the SF_6 is a very heavy molecule, it has a number of open inelastic channels. A conventional close-coupling calculation for e–SF_6 scattering is difficult and almost impossible to perform.

The independent atom model (IAM) [2] assumes that each atom scatters independently, neglects multiple scattering within the molecule, and assumes that any redistribution of atomic electrons due to molecular binding is unimportant. As a result, the theory of elastic scattering by a single molecule can be derived very simply from that for the separate atoms. The IAM with partial waves is a good approach which has been employed to calculate successfully the DCS, the integrated elastic and momentum transfer cross sections for e–CF_4 scattering [3,4] with a model potential method at intermediate energies. We use atomic units in this paper unless otherwise specified.

Based on the IAM [2], the differential cross section (DCS) averaged over all orientations of the molecular axis in the IAM is given by

[1] Address for correspondence.

PII S0375-9601(97)00318-6

$$I(\theta) = \sum_{i=1}^{N} I_i(\theta) + \sum_{i \neq j=1}^{N} f_i^*(\theta) f_j(\theta) \frac{\sin sr_{ij}}{sr_{ij}}, \quad (1)$$

where $I_i(\theta)$ and $f_i(\theta)$ are the atomic DCS and the scattering amplitude, respectively, appropriate to the ith atom in the molecule. r_{ij} and N are, respectively, the separation between the ith atom and jth atom, and the total number of atoms present in the molecule. s ($s = 2k \sin \frac{1}{2}\theta$) is the magnitude of the momentum transfer in the collisions. For the SF_6 molecule Eq. (1) reduces to

$$I_{SF_6}(\theta) = I_S(\theta) + 6I_F(\theta) \left(1 + 5\frac{\sin kr_{FF}}{kr_{FF}}\right) + 12(\mathrm{ASR} \cdot \mathrm{AFR} + \mathrm{ASI} \cdot \mathrm{AFI}) \frac{\sin kr_{SF}}{kr_{SF}}, \quad (2)$$

where S and F stand for sulphur and fluorine atoms, respectively. r_{FF} is the separation between the two fluorine atoms in the molecule which has been calculated by using the values of r_{SF} (bond length = $2.986a_0$) and the bond angle (90°). ASR, AFR and ASI, AFI are the real and imaginary parts of the scattering amplitude for the sulphur and fluorine atoms, respectively. The atomic scattering amplitude $f(\theta)$ in terms of partial waves is given by

$$f(\theta) = \frac{1}{2ik} \sum_l (2l+1)(S_l - 1) P_l(\cos\theta), \quad (3)$$

where S_l is the complex scattering matrix and can be obtained by solving the following radial equation using the method of partial waves,

$$\left(\frac{d^2}{dr^2} + k^2 - 2V_{opt}(r) - \frac{l(l+1)}{r^2}\right) u_l(r) = 0, \quad (4)$$

under the boundary condition

$$u_l(kr) \overset{r\to\infty}{\sim} kr[j_l(kr) - in_l(kr)] + S_l kr[j_l(kr) + in_l(kr)], \quad (5)$$

where $j_l(kr)$ and $n_l(kr)$ are the spherical Bessel and von Neumann function, respectively. $V_{opt}(r)$ is the appropriate complex optical potential which incorporates all the important physical effects,

$$V_{opt}(r) = V_s(r) + V_e(r) + V_p(r) + iV_a(r). \quad (6)$$

V_s, V_e, V_p and V_a are the static, exchange, polarization, and absorption potentials, respectively. In this paper, for the static potential $V_s(r)$ and the electron density function $\rho(r)$, we employ the analytical expressions of Salvat et al. [5], obtained by a fitting procedure to the Dirac–Hartree–Fock–Slater self-consistent data. They are given by

$$V_s(r) = -\frac{Z}{r} \sum_{i=1}^{3} A_i e^{-\alpha_i r}, \quad (7)$$

$$\rho(r) = \frac{Z}{4\pi r} \sum_{i=1}^{3} A_i \alpha_i^2 e^{-\alpha_i r}. \quad (8)$$

A_i and α_i are the parameters tabulated in Ref. [5]. The forms of V_e, V_p, and V_a have been presented in Ref. [6].

The integrated elastic and momentum transfer cross sections are obtained, respectively, from the following relations,

$$Q_I(E) = 2\pi \int_0^{\pi} I(\theta) \sin\theta \, d\theta, \quad (9)$$

$$Q_M(E) = 2\pi \int_0^{\pi} I(\theta)(1 - \cos\theta) \sin\theta \, d\theta. \quad (10)$$

In this Letter, employing the IAM along with an optical potential we calculate first the DCS, integrated elastic and momentum transfer cross sections of e–SF_6 scattering at 100, 150, 200, 300, 500 and 700 eV. The limit of l_{max} in Eq. (4) is taken to be 50. An effective-range formula,

Table 1
The integrated elastic (Q_I) and momentum transfer cross section (Q_M) for electron scattering by SF_6 molecules (in units of a_0^2); the experimental results are from Ref. [8]

E (eV)	Q_I		Q_M	
	present results	experiment	present results	experiment
100	96.76	66.78	21.86	20.36
150	72.84	55.71	13.36	15.61
200	59.87	46.78	19.26	10.64
300	45.51	37.85	15.83	16.29
500	30.48	27.11	13.03	13.64
700	21.39	21.5	11.97	12.34

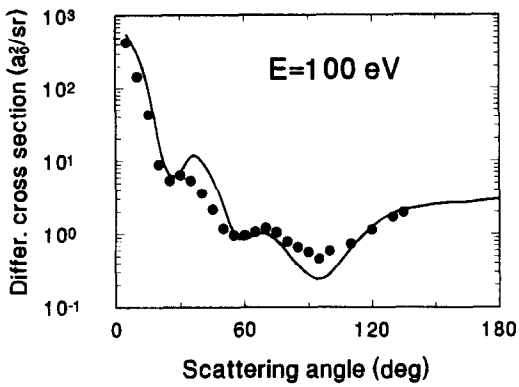

Fig. 1. Elastic different cross sections for e–SF_6 scattering at 100 eV. Solid curve: present results. (•) Experimental data from Ref. [8].

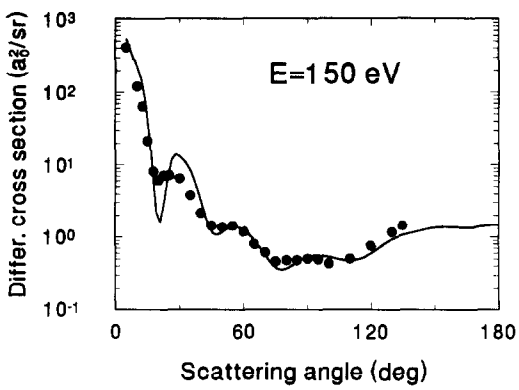

Fig. 2. Same as in Fig. 1, but for 150 eV.

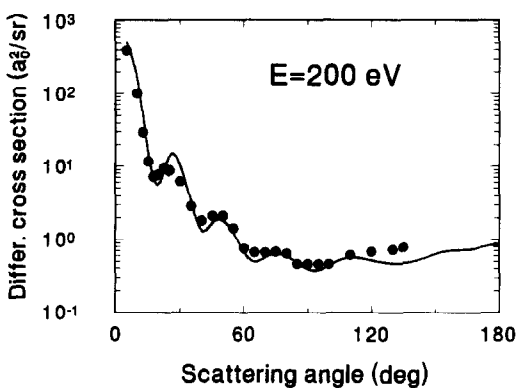

Fig. 3. Same as in Fig. 1, but for 200 eV.

$$\tan\delta_l = \frac{\pi\alpha k^2}{(2l+1)(2l+3)(2l-1)}, \qquad (11)$$

is used to generate the higher partial-wave contributions until again a convergence of less than 0.5% is achieved in the DCS, the integrated elastic and momentum transfer cross sections. To our knowledge, Sakae and coworkers [8] found the DCS, the integrated elastic and momentum transfer cross sections from experiments, and there are no other theoretical calculations at these energies. Our results are shown in Figs. 1–6 and Table 1, and are compared with the measurements of Sakae et al.

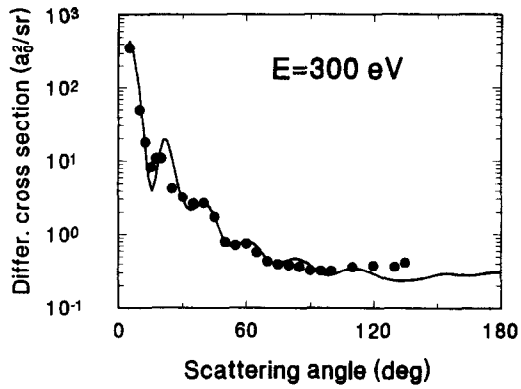

Fig. 4. Same as in Fig. 1, but for 300 eV.

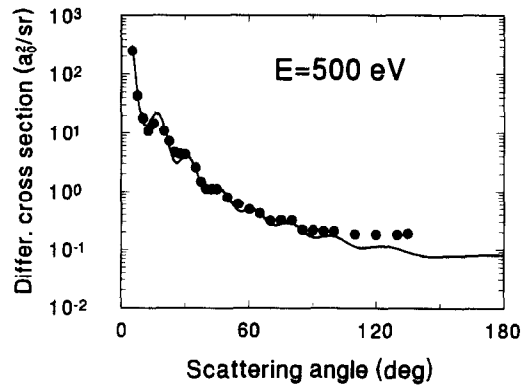

Fig. 5. Same as in Fig. 1, but for 500 eV.

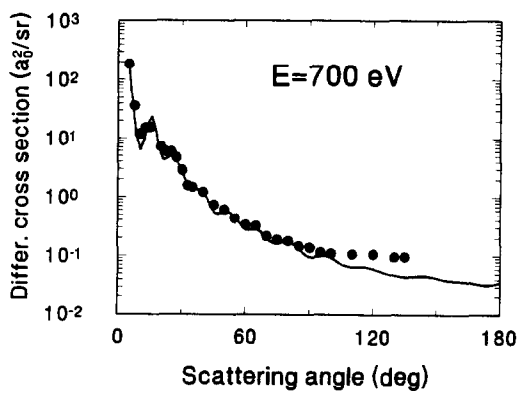

Fig. 6. Same as in Fig. 1, but for 700 eV.

From Fig. 1 at 100 eV, we see the present results of the DCS reproduce the qualitative behavior of the experimental data of Sakae et al. and are in agreement with the measurements at intermediate angles. It is evident that there is fairly good agreement between the present results and the experimental data in Figs. 2–6. Our DCS results give the same position and depth of the DCS dip as experimental data at $E \geqslant 200$ eV except for the first dip in Fig. 2 and Fig. 4, where they are deeper than the corresponding experimental data. In Figs. 1–6 we notice that the present results are in quite good agreement with the measurements as the incident energy increases at small scattering angles. On the other hand, our present results are about 5–20% lower than the measurements at larger angles ($120° < \theta < 135°$) at 100–300 eV. Moreover, the discrepancy rises to about 10–50% as the incident energy is increased (at 500 eV and 700 eV). In this regard, it may be noted that the present imaginary part of the optical potential is known to overestimate the flux loss to the excited electronic states for large scattering angles, particularly at high incident energies, and hence the underestimation of the DCS is according to our expectation [9]. Figs. 4–6 show that, at large incident energies, the $\sin sr_{ij}$ terms oscillate rapidly, resulting in more structure in molecular DCS at larger angles. For small angle scattering, our results are slightly higher than the measurements of Sakae et al. This is because the IAM neglects the multiple scattering and the valence bond distortion which are known to cause a decrease in the cross sections [10].

Table 1 shows that the present Q_I results are higher than the measurements of Sakae et al. in the range 100–500 eV and merge well with the experimental data as the incident electron energy increases. For example, at 100 eV and 300 eV our Q_I are about 43.8% and about 12.4% higher, as compared with the data of Sakae et al., respectively. For Q_M, the present calculations are within about 15% of the experimental data, and are in good agreement in the whole energy range. The underestimation of Q_I at 700 eV and Q_M in 150–700 eV is again probably due to the larger flux loss to the excited electronic states as mentioned above.

Employing IAM, we also calculate the DCS, integrated elastic and momentum transfer cross sections for electron scattering from CF_4. Our results are in good agreement with the measurements of Sakae et al. [11]. The calculation results of the DCS, the integrated elastic and momentum transfer cross sections for e–SF_6 scattering employing the IAM and local optical potential, obtained in this Letter, are promising. We may consider this approach as a successful attempt using the IAM to transform the molecular scattering problem into an atomic scattering problem which is easier to handle, in particular at higher incident energies. Though this method cannot lead to very exact calculations, the present results compare qualitatively well. They predict the outcome of experimental research, particularly for these molecules of which the wave functions are not available at present. Without such wave functions no theoretical calculations can be carried out. We also hope that the IAM can lead to more experimental work and theoretical calculations in the intermediate- and high-energy region, in the near future.

This work is supported by the Science Foundation of the Henan Province, China.

References

[1] L.G. Christophorou, Electron–molecule interactions and their applications, Vols. 1 and 2 (Academic Press, New York, 1984).
[2] H.S. Massey, Electronic and ionic impact phenomena, Vol. 2 (Clarendon, Oxford, 1969).
[3] D. Raj, J. Phys. B 24 (1991) L431.
[4] S.P. Khare, D. Raj and P. Sinha, J. Phys. B 27 (1994) 2569.
[5] F. Salvat, D.J. Martinez, R. Mayol and J. Parellada, Phys. Rev. A 36 (1987) 467.
[6] Y.H. Jiang, J.F. Sun and L.D. Wan, Phys. Rev. A 52 (1995) 398.
[7] X.Z. Zhang, J.F. Sun and Y.F. Liu, J. Phys. B 25 (1992) 1893.
[8] T. Sakae, S. Sumiyoshi, E. Murakami, Y. Matsumoto, K. Ishibashi and A. Katase, J. Phys. B 22 (1989) 1385.
[9] G. Staszewska, D.W. Schwenke, D. Thirumalai and D.G. Truhlar, Phys. Rev. A 28 (1983) 2740.
[10] S. Hayashi and K. Kuchitsu, Chem. Phys. Lett. 41 (1976) 575.
[11] Y.H. Jiang, J.F. Sun and L.D. Wan, in preparation.